SNOWDRIFTS AND THE AERODYNAMIC DRAG ON SCALED-MODEL SHELTERBELTS

R. A. Schmidt[1], R. L. Jairell[2], and R. D. Tabler[3]

ABSTRACT

This paper reports the design and initial testing of a device that measures the wind force on model windbreaks. Our objective is to improve understanding of the relationship between shelterbelt porosity, aerodynamic drag, and snowdrift formation. Two identical drag-boards allow simultaneous comparison of drag on a model shelterbelt with drag on a snow fence model for which the prototype drag coefficient is known.

INTRODUCTION--POROSITY AND DRAG

Porosity ratio, the fraction of openings to frontal area perpendicular to the wind, is useful for predicting snow fence drifts. Fences of 50% porosity maximize snow storage (Tabler 1994). However, a solid fence (0% porosity) creates a larger upwind drift than a fence of equal height with 50% porosity. Porosity also predicts aerodynamic drag for 2-dimensional obstacles. A drag coefficient C_h is defined by the wind speed U_h at the height h of the obstacle, without the object present. If the drag force per unit length of obstacle is D, then $C_h = D/0.5\rho U_h^2 h$, where ρ denotes air density. For unobstructed flow described by the logarithmic wind profile, the reference velocity is $U_h=(u_*/k)\ln(h/z_0)$. Here, u_* is friction velocity, z_0 is roughness parameter, and k=0.4 is von Karmen's constant. Guyot (1978) and Taylor (1988) review drag studies that apply to windbreaks (Fig. 1). Tabler (1994) includes drag measured on a full-scale fence (Fig. 1).

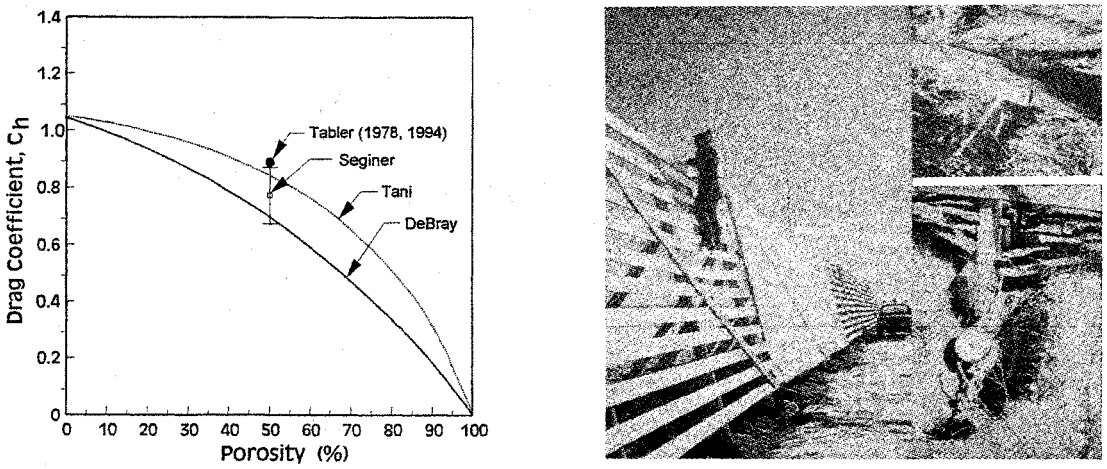

Figure 1. Drag coefficients decrease with increasing porosity of 2-dimensional obstacles like snow fences. Guyot (1978) and Taylor (1988, Fig. 3) give the references. Photos at right show the setup for full-scale measurements of drag force on a snow fence (Tabler 1978, 1994). Sills of one fence panel were set on angle-iron fulcrums. Observers recorded maximum forces on the windward anchors and corresponding wind gusts at 10-m height.

Shapes of snowdrifts around shelterbelts (tree rows) are notably different than drift shapes created by snow fences. Drifts upwind of shelterbelts usually contain more snow than those upwind of snow fences (see Schmidt and Jairell, 1994, this volume). To design shelterbelts that effectively reduce windspeeds and control drifting, we must understand how shelterbelt characteristics determine these deposition differences.

Predicting drift shapes from shelterbelts porosity is complicated by two factors: (1) porosity is not uniform with height, and (2) elements of the shelterbelt (trees) are

[1,2]Hydrologist and Hydrologic Technician, respectively, Rocky Mountain Forest and Range Experiment Station, 222 S. 22nd Street, Laramie, WY 82070. (307)742-6621.
[3]Consultant in Snow and Wind Engineering, Tabler & Associates, P.O. Box 483, Niwot, CO 80544-0483. (303)652-3921.

Presented at the 62th Western Snow Conference, April 18-21, 1994, Santa Fe, New Mexico.

arranged in a 3-dimensional pattern, compared to the more 2-dimensional array of boards on the face of a snow fence. Air flow seeks a path of least resistance through the shelterbelt. The utility of optical measurements of porosity is questionable (Bean et. al. 1975, p. 428). Is there a shelterbelt characteristic that better describes its drag?

METHODS--DRAG BOARD DESIGN

The many variations of shelterbelt structure, and difficulties in full-scale drag measurements, make small-scale models a tempting experimental option. Using Tabler's (1978) drag coefficient for a 3.8-m-tall, 50% porous fence, we estimated the drag force on a 1:30 scale model snow fence, 12.5-cm tall. At the reduced wind speeds required for proper dynamic scaling, computed drag on a 91-cm-long model fence ranged from 50 to 250 g.

We built two "identical" devices to measure model drag force. Each began as a 1.2-by-2.4-m (4-by-8-ft) sheet of 19-mm (3/4-in) plywood. A 15-by-91-cm (6-by-36-in) rectangular opening cut in the center had its long axis aligned with the sheet. Ball-bearing drawer guides were modified to provide a carriage for 6.4-mm (1/4-in) aluminum plates that fit in the openings, flush with the top surface of the plywood sheet (Fig. 2). The test plates fit over pins on the carriage, allowing plates to be interchanged. Clearance around the plate was approximately 2 mm. Sheet metal strips inlaid on each end of the test plate opening facilitated attaching models with magnetic bases. Enclosing the carriage and load cell reduced exposure to dirt.

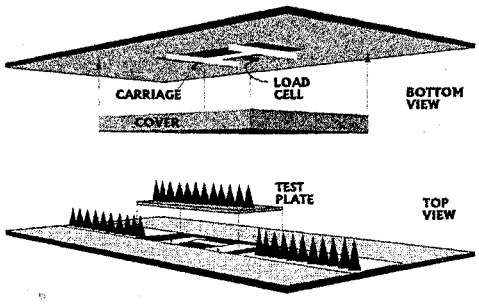

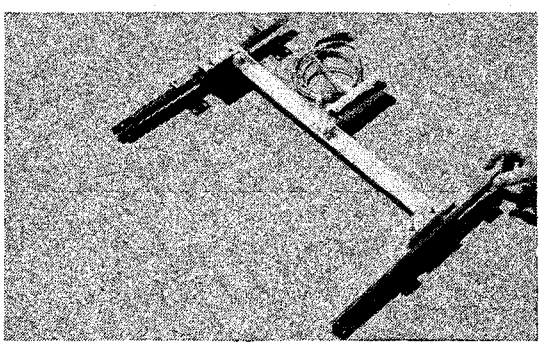

Figure 2. Perspective drawing of the drag board and details of the carriage.

A lever arm that contacted the center of the carriage transferred drag force to the load cell (Fig. 2). The lever provided an adjustable mechanical advantage, increasing the load cell's 60-g range by 3 to 5 times. We removed most of the ball-bearings in the drawer guides and replaced all grease with a dry graphite lubricant to reduce friction. Calibration with a spring scale (Fig. 3) provided plots such as Figure 4. A data logger connected by modem and cable to a computer in a mobile laboratory read the load-cell outputs 5 times each second. Readings requested by the computer each second were saved each minute in disk files.

Seven cup-type anemometers measured the vertical profile of mean horizontal wind speed (Fig. 5). A second data logger transferred 1-min profiles to computers in the mobile laboratory by radio link. An array of four heated-bead anemometers provided fast-response wind speeds just above the drag board (Fig. 6). Signals from these sensors plus wind direction and speed at 1-m height by a propeller-vane were read each second with the load cell signals.

RESULTS--INITIAL TESTS

A soccer field on the University of Wyoming campus, Laramie, provided a limited fetch over short grass (Fig. 7). We placed the drag boards on a frame and used Masonite sheets and duct tape to build a transition from the fetch to the model boards. Load cell calibrations were repeated after the drag boards were set and leveled. Wind direction was south to southwest during our first tests on the afternoon of 22 March 1994. Based on the forecast, our setup was for winds more westerly than those that occurred during most of that afternoon. Temperatures ranged from a high of 17°C at noon to 11°C at 1800h. Wind profiles showed a roughness parameter, z_0, near 1 cm for the grass fetch.

Initial tests used the 12.5-cm Wyoming Standard Plan snow fence model as a reference, because the drag coefficient of the full-sized fence is known. Other models included single- and double-row shelterbelts, and scaled-model snowdrifts (Fig. 8).

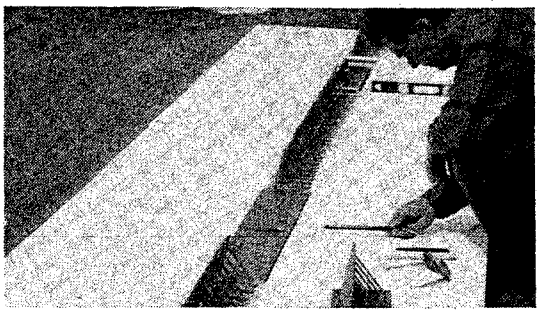

Figure 3. We calibrated the drag boards after leveling, by applying loads to a bare test plate with a spring scale.

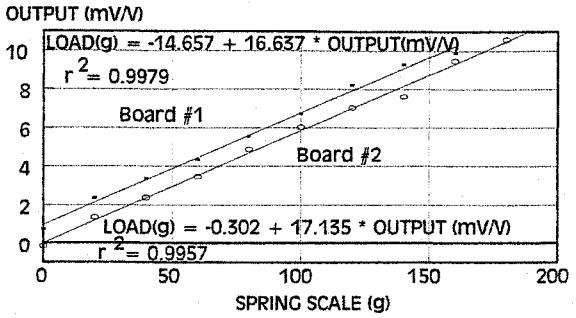

Figure 4. Drag board calibrations were plotted after each releveling. Although slopes remain constant, offsets changed.

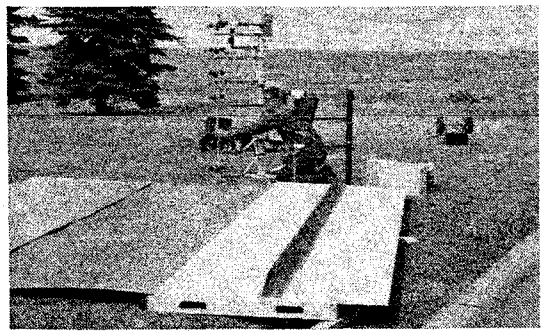

Figure 5. Mean wind speed profiles were measured by cup anemometers and a data logger that transmitted results to the mobile laboratory.

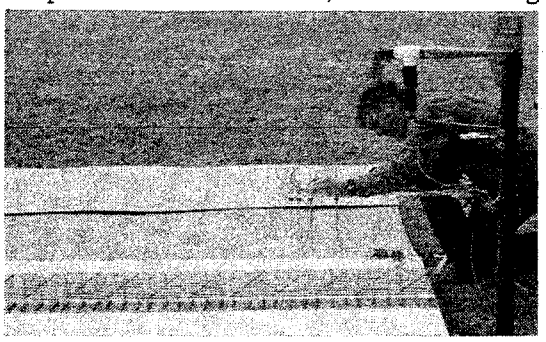

Figure 6. Heated-bead anemometers provided four fast-response wind speeds in a profile between the surface and the height at the top of the model.

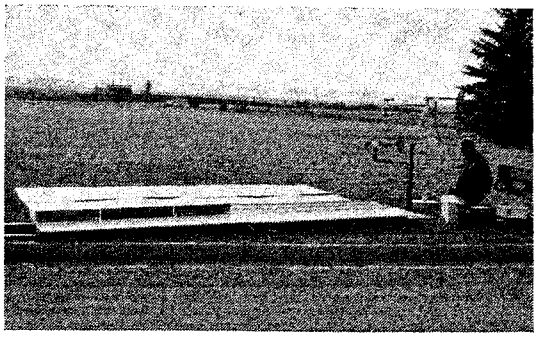

Figure 7. We conducted initial testing on a soccer field at the UW campus. The fetch was unobstructed over grass for only 50-100 m.

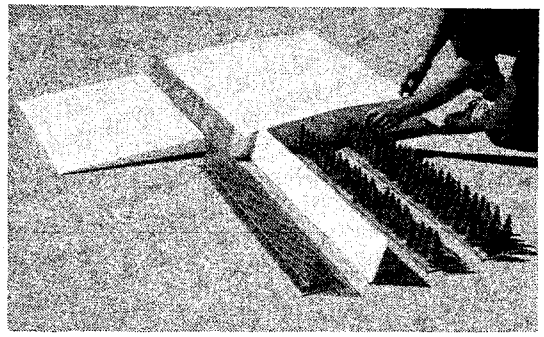

Figure 8. Models initially tested included 50% porous, and solid snow fences, single and double tree rows, and a fence with a model snow drift.

Image analysis produced vertical profiles of porosity ratio for the model shelterbelts (Fig. 9). For example, the single tree-row model had an overall porosity ratio of 42%, but the top third of the model, where wind speed is greater, has porosity of more than 50%. This probably explains the initial drag-board results showing the single tree row with a drag coefficient similar to the 50%-porous snow fence (Fig. 10).

The drag coefficient of each model is evaluated from a regression of the drag force (measured by the load cell) on the dynamic force ($0.5\rho U_h^2 h$). Differences in time response between the wind speed sensor and the drag-boards produce scatter in the data. In Figure 10, points are 7-s running averages for readings when wind direction was within 7 degrees of perpendicular to the models.

Tests on 22 March 1994 showed that design calculations gave the correct force range. Test plates are heavy enough to cause changes in load cell zero with slight deviations from level. Although this does not affect the estimation of drag force, it may limit the range. We will add a method of making fine adjustments to the carriage level after the boards are leveled. These first results encouraged us to pursue this method for exploring the relationship between shelterbelt porosity, aerodynamic drag, and snowdrift formation.

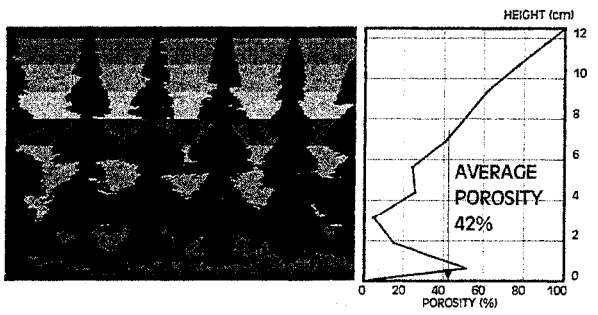

Figure 9. Image analysis produced vertical profiles of porosity for shelterbelt models. An example is this 10 level plot for the single-row tree model.

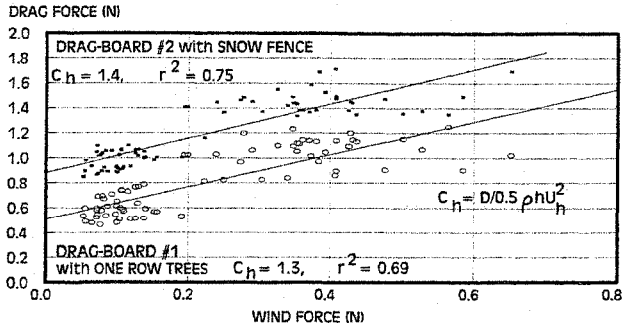

Figure 10. Initial drag-board comparison indicated that the single-row tree model (42% mean porosity), had a drag coefficient similar to the snow fence (50%). Data are 7-s running means.

REFERENCES

Bean, Allan, Alperi, R. W. and C. A. Federer. 1975. A Method for Categorizing Shelterbelt Porosity. Agricultural Meteorology 14:417-429.

Guyot, G. 1978. Determination des efforts exerces par la vent sur un brise-vent. Boundary Layer Meteorology 15:57-67 (in French, with English abstract).

Hagen, L. J. and E. L. Skidmore. 1971. Windbreak Drag as Influenced by Porosity. Trans. ASAE (1971) 464-465.

Jairell, Robert L. and R. A. Schmidt. 1990. Snow Fencing Near Pit Reservoirs to Improve Water Supplies. Proceeding, 58rd Annual Western Snow Conference (Sacramento, CA, April 17-19, 1990), pp. 156-159.

Jairell, Robert L. and R. A. Schmidt. 1987. Constructing Scaled Models for Snowdrift Tests Outdoors. Proceeding, 55rd Annual Western Snow Conference (Vancouver, British Columbia, Canada, April 14-16, 1987), pp. 166-169.

Jairell, Robert L. and Ronald D. Tabler. 1985. Model Studies of Snowdrifts Formed by Livestock Shelters and Pond Embankments. Proceeding, 53rd Annual Western Snow Conference (Boulder, CO, April 16-18, 1985), pp. 167-170.

Schmidt, R. A. and Robert L. Jairell. 1994. Instantaneous Measurements of Snowdrifts in Small-scale Modeling Proceeding, 62nd Annual Western Snow Conference (Santa Fe, New Mexico, USA, April 18-21, 1994), (this volume).

Tabler, R. D. 1978. Measured Wind Loads on 50% Porous Snow Fences. Third U.S. National Conference on Wind Engineering Research, (Feb. 26-Mar. 1, 1978, Gainesville, Florida), Wind Engineering Research Council and National Science Foundation. Preprint Vol., p. III-27-1.

Tabler, Ronald D. 1980. Self-Similarity of Wind Profiles in Blowing Snow Allows Outdoor Modeling. Journal of Glaciology 26(94): 421-434.

Tabler, Ronald D. 1994. Design Guidelines for the Control of Blowing and Drifting Snow. Strategic Highway Research Program, Publication SHRP-H-381, National Research Council, Washington, DC. 364 pp.

Tabler, Ronald D. and Robert L. Jairell. 1980. Studying Snowdrifting Problems with Small-Scale Models Outdoors. Proceeding, 48th Annual Western Snow Conference (Laramie, WY, April 15-17, 1980), pp. 1-13.

Taylor, Peter A. 1988. Turbulent Wakes in the Atmospheric Boundary Layer. In Steffen, W. L. and O. T. Denmead (eds.) Flow and Transport in the Natural Environment: Advances and Applications, Proc. of an Int. Symp., Canberra, 1987. Springer-Verlag, New York, 270-292.